# Study of the Refractory Materials for the Progress of the Vacuum Interrupters

Shaker J. Gatan
Riga Technical University, Azenesiela 12/1, Riga LV-1048
Latvia
{Shaker.gatan@outlook.com}

***ABSTRACT:*** *Refractory materials are used to study the progress of the vacuum interrupters. The alloys are capable of passing currents and chopping currents and are transient over voltages. The normal designing switchers are using the same classical steps of atoggle ways. Using the application of medium voltage switching techniques we have presented the sequence of the switching process time for a static switching process. These are applied for power electronics which are designed for RF systems and protect the circuit applications.*

**Keywords:** Calculating Chopping Currents, Damping Circuit, LTT Thyrsitors, Sequences of Switching Times, MATLAB/ Simulink

**Received:** 18 Februrary 2021, Revised 30 May 2021, Accepted 9 June 2021

**DOI:** 10.6025/ed/2021/10/2/52-59



## 1. Introduction

Circuit breakers using different media for interrupting currents may exhibit different characteristics with respect to all of the primary functional requirements of the breaker. Each type of circuit breaker has a unique set of characteristics which must be thoroughly understood before the breaker can be applied with correctly designing and confidence by considerations of arcing currents, chopping currents, over voltage transients, multiple re-ignitions, voltage escalation and high frequency which calculate for full load during processing switching time.

Both of hybrid application and damping circuit theory have been offered a smooth process switches which consists of high speed mechanical contact with power semiconductors as diverting switching, its an excellent performance in limiting chopping current. In hybrid switch system, the mechanical contact conducts large current with low losses, [1], [2], and [10].

## 2. Analysing Damping Circuit

### 2.1 The vacuum interrupter involves very large number of practical transients problems in power system of medium voltage switching process

The analysis shows that the effect of damping an oscillatory circuit can be described in terms of a single parameter, designed $\eta$, or its reciprocal λ, which is the ratio of the resistance to the surge impedance of the circuit i.e;

$$\eta = \frac{R}{Z} = \frac{R}{\sqrt{L/C}} \tag{1}$$

This fact permits the construction of generalized damping curves for different values of $\eta$, from which the solutions to many practical problems can be extracted with about the same effort as one expand by using a table of logarithms.

Normally our analysis for the switching process basically on parallel *RLC* circuit as following;

*L* - indicative load of stator winding coils;

*C* - parallel parasite‘s capacitors;

*R* - evaluating resistance that can be damping oscillating.

$$i_L(s) = \frac{V(0)}{L} \cdot \frac{1}{s^2 + \frac{s}{T_p} + \frac{1}{T^2}} \tag{2}$$

$$L^{-1} \frac{1}{s^2 + \frac{s}{T_p} + \frac{1}{T^2}} \tag{3}$$

From Eq. (3) express in dimensionless from the current in the inductor of any parallel *RLC* circuit, with any degree of damping. We note that the only parameter involved is $\eta$.

So that a family of generalized curves can be drawn from Eq. (3) for different values of $\eta$ with dimensionless quantity, t`, as abscissa. This has been done in Figure 1.

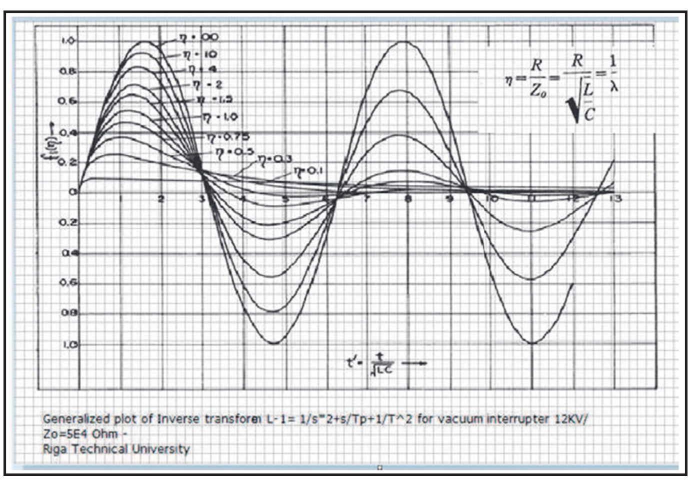


Figure 1. Generalized plot of inverse transform

Where $\eta = 0.5$, the sine function changes from a circular to a hyperbolic function. We might have developed the curves for this condition, following the same argument. By calculating the inductor current in parallel *RLC* circuit under conditions of a subsidence transient, but have a far wider application. However to gain familiarity with these curves, consider a specific example where the inductor current is required in a circuit in which the components have the following values:

$R = 10^5\ \Omega$, $L = 5\text{H}$, $C = 2 \cdot 10^{-8}\ \text{F}$.

These values are typical of unloaded transformer, where $R$ represents the equivalent loss resistance. Suppose $Vo = 13.8\sqrt{2}$ KV *So.* $Zo = \sqrt{L/C} = 5\cdot 10^4\ \Omega$, $\eta = 2$. The curve labelled $\eta = 2$ in Figure 3 gives the shape of the current we are looking for.

### 2.2 Parallel Switching Technique

The resistor application technique $R$ circuit will be diminished the amplitude of the first peak value of chopping current , if we connect this circuit as parallel application with two electrodes – parallel operation mode [1]

The flexible rates for transition of $du / dt$ and $di / dt$ between to elements such as electroplates and set of thyristors. Flexible $du / dt$ and $di / dt$ [6]-[9] for the set of thyrsitors as a control techniques are presented in Simulink models. It propos to make a diverting of the chopping currents after the time of ionization by using a damping resistance circuit.

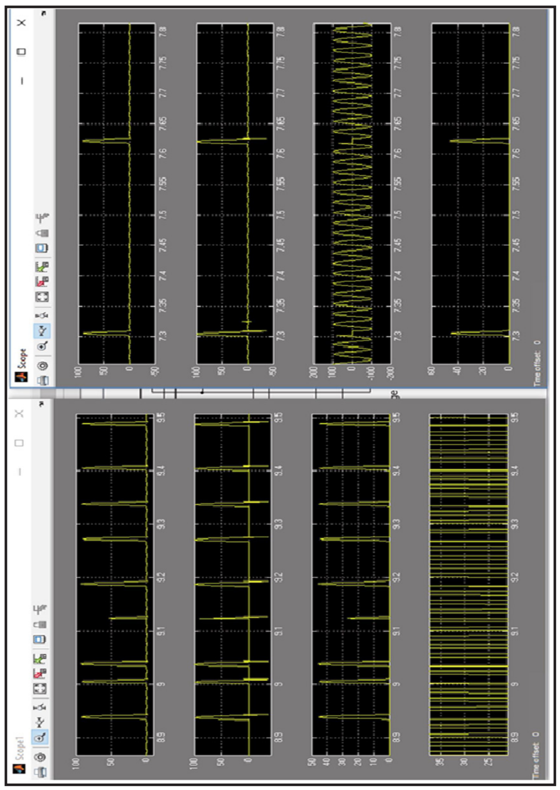

Figure 2. $di / dt$ and $du / dt$ alignment between electroplates and thyristor

## 3. Switching Transition Rates

Vacuum interrupter involves by switching transition rates of $di / dt$ and $du / dt$ conversion. An Experiment synthetic figure which describes the test circuit an arc of a few thousand amperes is drawn between a pair of separating contact *"synthetic prototype"* with a sealed vacuum interrupter.

Current commutation is typically achieved within 20 *us*. The circuit subsequent applies a fast-rising transient recovery voltage across the gap. by adjusting circuit parameters it is possible to cause the switch to re-ignite. A mathematical model which analyzes events during the commutation period and the recovery period afterwards has been proposed by Childs and Greenwood [8]. Two time periods are defined in the mathematical model: a commutating period prior to current zero and post arc time. The model has been used to calculate the post arc current and transitions time $di / dt$ and $du / dt$ were calculated according to following formula.

$$di / dt = I_{ss}/t_r \tag{4}$$

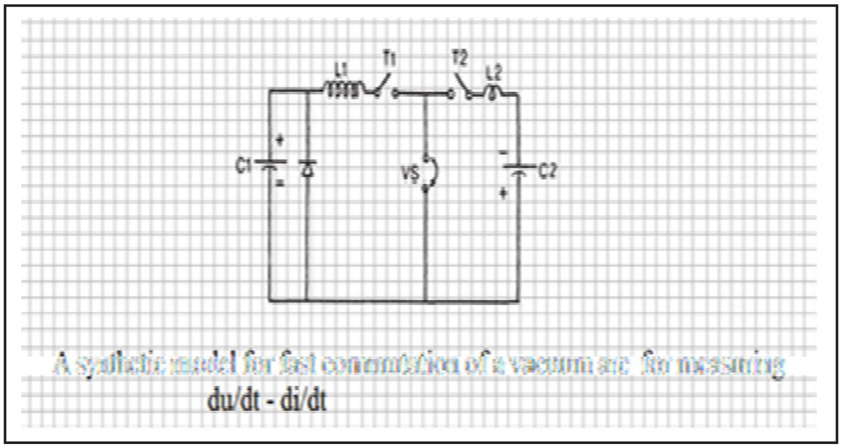


Figure 3. A Synthetic experiment for fast commutation of a vacuum arc

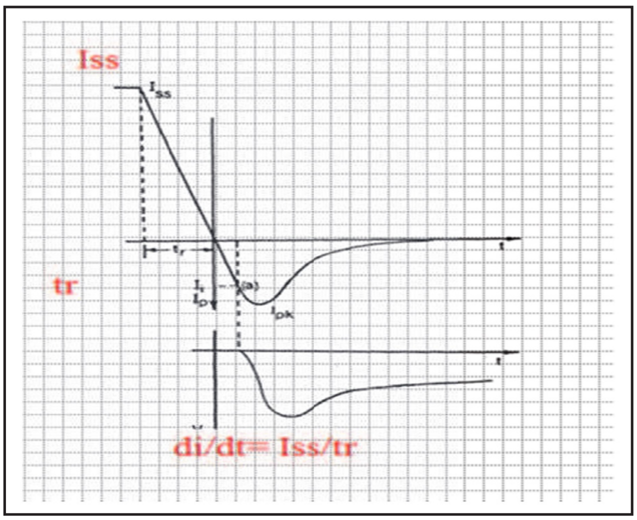


Figure 4. Transition process *di* / *dt* and *du* / *dt* for TRV

The vacuum switch under test *VS* has its contacts open at short fixed gap; the gap selected was in the range (100-150 mm). The capacitor *C*1 is charged until the gap of *VS* sparks over, at which time C1 delivers an oscillatory current to the gap. The fixed gap assures a reasonably constant breakdown voltage ( ~ 15KV). *dI* / *dt* is controlled by *L*1. The TRV frequency is adjusted by C2 (<<C1) as it resonates with *L*1. The ranges of values chosen during the course of the test were; $I_{SS}$ = 1.0KA, 2.0KA, 3.0KA, 4.0KA & 5.0KA. The twenty nine shots were made to calculate *di* / *dt* and *du* / *dt* with several test were for each ramp down time; the results are summarized in Table 1.

$I_{SS}$ - the steady state current being commutated,

*tr* - the ramp down us,

*dI* / *dt* - the average rate of current decline during current commutation as given by *Iss* / *tr*, *Q* - the average integrated post- arc current,

*du* / *dt* - the average rate of rise of recovery voltage, being computed from the slope of the linear portion of the re-covery voltage,

*I peak* - arc current,

*V*2 - charging voltage on the commutating capacitor.

| Iss KA | tr µs | di/dt A/ µs | Q | du/dt | $I_{pk}$ | V2 KV |
|---|---|---|---|---|---|---|
| 1.0 | 7.8 | 128 | 9.4 | 1.2E10 | 22 | 2.0 |
| 1.0 | 6.9 | 145 | 18.2 | 1.2E10 | 30 | 2.25 |
| 1.0 | 6.13 | 163 | 21.3 | 1.2E10 | 38 | 2.5 |
| 1.0 | 5.06 | 197 | 28.3 | 1.2E10 | 44 | 3.0 |
| 1.0 | 4.32 | 232 | 38.3 | 1.2E10 | 60 | 3.5 |
| 1.0 | 3.77 | 266 | 49.7 | 1.2E10 | 67 | 4.0 |
| 1.0 | 3.34 | 299 | 49.7 | 1.2E10 | 67 | 4.5 |
| 2.0 | 10.9 | 183 | 17.1 | 1.9E10 | 32.5 | 3.0 |
| 2.0 | 9.1 | 221 | 29.3 | 1.9E10 | 44.5 | 3.5 |
| 2.0 | 7.8 | 256 | 42.8 | 1.9E10 | 53.0 | 4.0 |
| 2.0 | 6.9 | 291 | 57.0 | 1.9E10 | 67.0 | 4.5 |
| 2.0 | 6.13 | 326 | 67.0 | 1.9E10 | 75.5 | 5.0 |
| 2.0 | 5.55 | 361 | 80.0 | 1.9E10 | 80.0 | 5.5 |
| 3.0 | 12.6 | 237 | 27.5 | 1.2E10 | 40.75 | 4.0 |
| 3.0 | 11.5 | 261 | 43.0 | 1.2E10 | 54.3 | 4.3 |
| 3.0 | 10.5 | 275 | 48.0 | 1.2E10 | 63.0 | 4.5 |
| 3.0 | 10.1 | 295 | 34.5 | 1.2E10 | 68.0 | 4.75 |
| 4.0 | 16.3 | 245 | 15.5 | 1.2E10 | 30.0 | 6.0 |
| 4.0 | 14.9 | 268 | 18.5 | 1.2E10 | 36.5 | 6.0 |

Table 1. Calculation of mechanical switching transition rates

The results we have obtain that are the sequence of test with progressively ramp down time as Fig. 6. The transition rates of $du / dt$ is approximately constant **1.2E10** V/s, because that explains the materials Alloys (CU-CR-70) is a constant transition rate but the transition rates of $dI / dt$ is changed for average values (128 A/us up to 268 A/us for the $I_{SS}$ 5.0 KA). This indicates both of the similarity functional with power electronics transition rates and Logical consistency for my currently research with Simulink experiments also.

**4. Flow Chart & Single Line Diagram**

Flexible rates among electroplates and sets of thyristors are a new control techniques to achieve

1) Independent control of the out put terminals between two components $du / dt$ and $di / dt$ rates that adjusted *electronically* over a wide range without electromagnetic interference EMI and voltage overshoots and

2) Maximum compatibility with integrated M.V circuit techniques

**5. Conclusions**

1. The static capacitors are always interactive with the switching process – Inherited capacitors for each process unit function.

2. Many researching papiers indicate that the chopping current will not increase more that 5A – first peak value for most full load operation with all types of M.V synchronous motors.

3. Further measurement shall be implemented for determine the maximum values of discharged static capacitance.

4. The theory of rectifying chopping currents and dissipated energy thorough the resistor will be offer the static switching process.

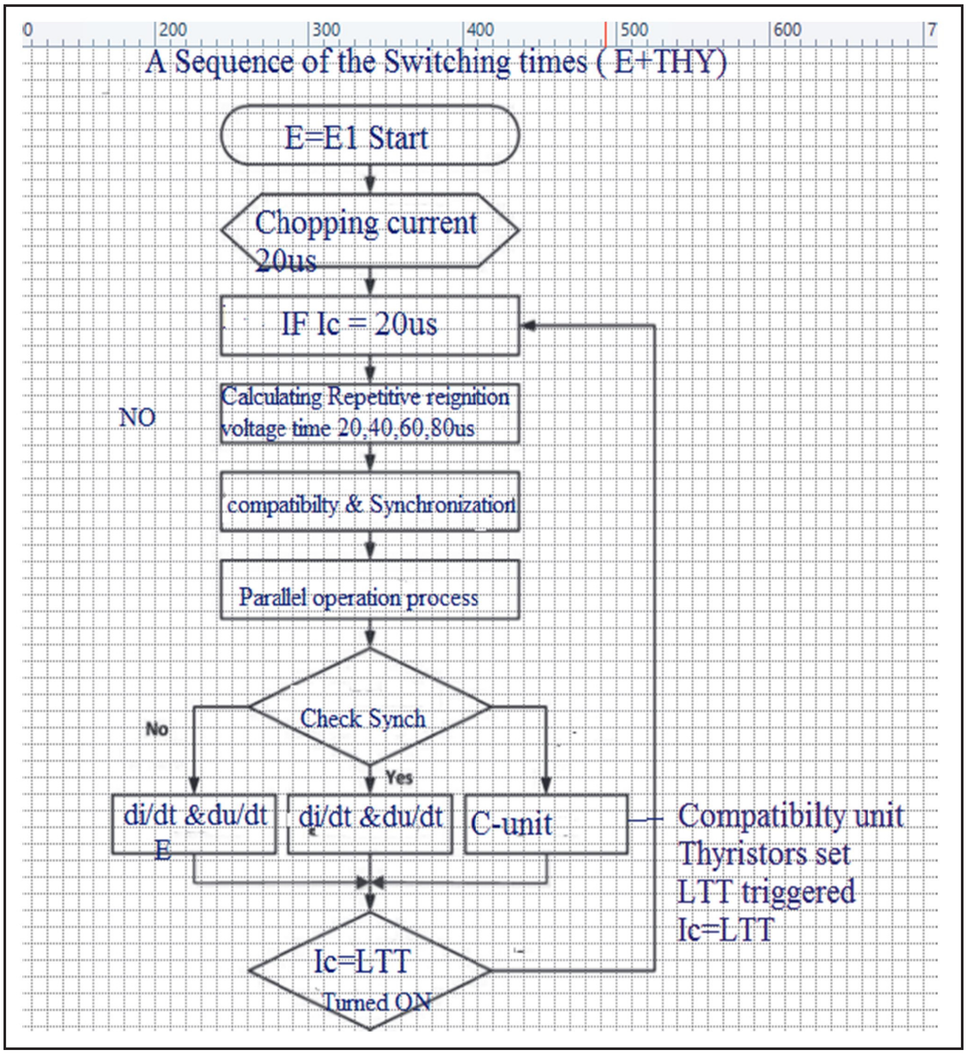


Figure 5. Algorithmic application for turned ON process of parallel operation mode

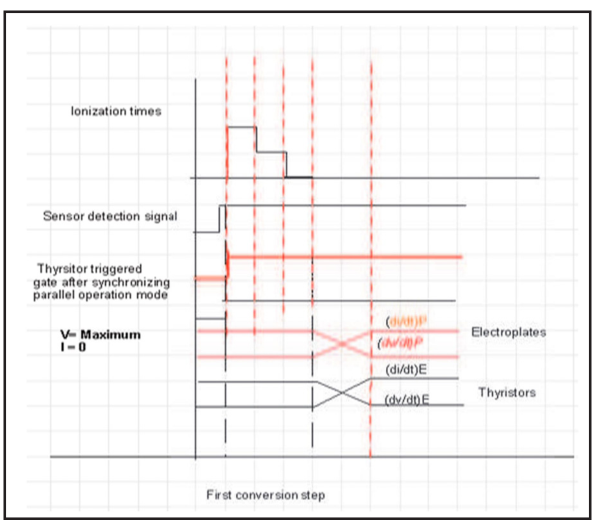


Figure 6. Algorithmic switching times for turned – ON process

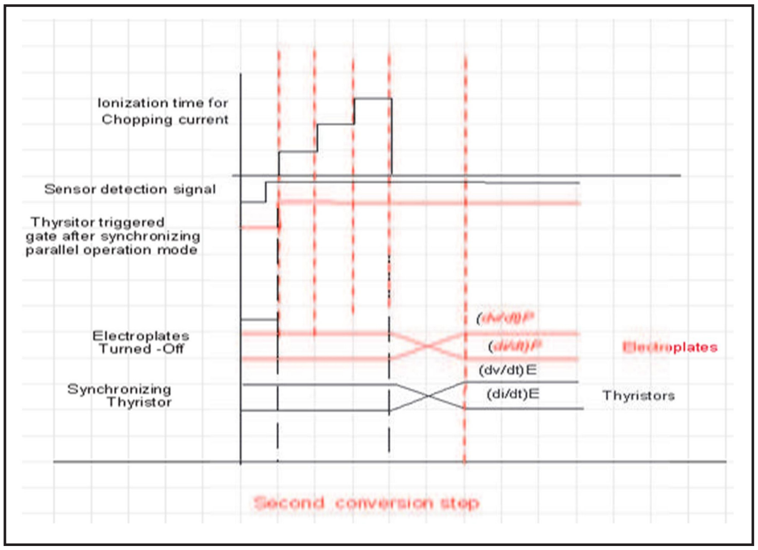


Figure 7. Algorithmic switching times for turned – OFF process

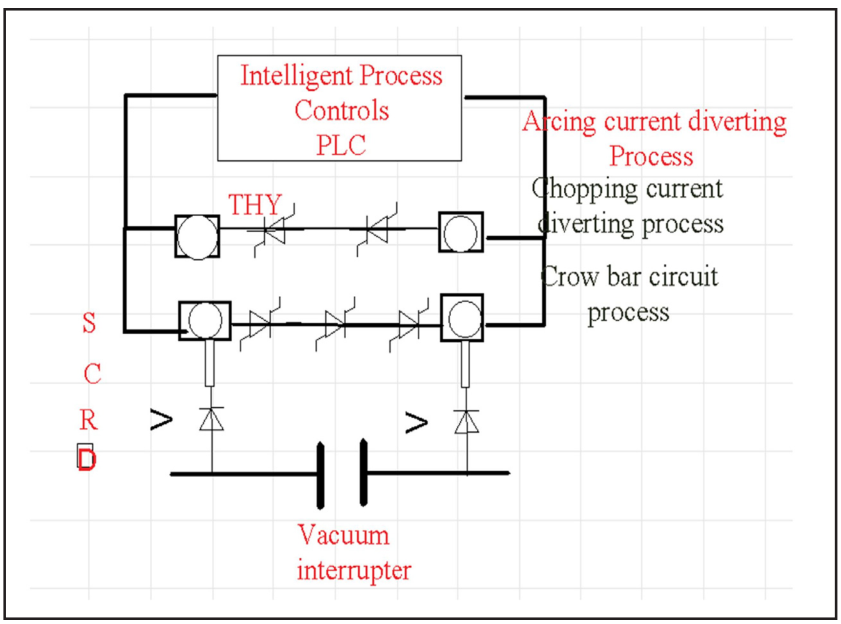


Figure 8. A single line diagram of a compact design of a new proposal of vacuum interrupter for medium voltage switching

## References


[1] Gatan, S. (2016). Synchronizing Switching Times of Vacuum Interrupters for Medium Voltage, *IEEE*, 19-20*th* September 2016, Lodz university of Technology Lodz-Poland.

[2] Murano, M., Yanabu, S., Ohashi, H., Ishizuka, H., Okazaki, T. (1977). Current Chopping Phenomena of Medium Voltage Circuit Breakers, *IEEE Trans. on Power Apparatus and Systems,* vol. PAS-96, p. 143-149.

[3] Holmes, F. A. (1974). An Empirical Study of Current Chopping by vacuum Arcs, paper C 74088-1, *IEEE PES Winter Meeting*, New York, (January).

[4] Greenwood, A. N. (1960). The Effect of Current Chopping in Circuit Breaker on Networks and Transformers, part II,

*Trans. AIEEE*, vol. 79, part III, p. 545-555.

[5] Tuohy, E. J., Panek, J. (1977). Chopping of Transformer Magnetizing Currents: part I; Single Phase Transformers", paper No. F77 096-1, *IEEE PES Winter Meeting*, New York, (February).

[6] High Power Directed–light–Triggered Thyrsitor valve Technology. The Basis for Advanced Power Electronics, Solutions in Transmission Systems – SIEMENS.

[7] Childs, S. E., Greenwood, A. N. (1983). Events Associated with Zero Current Passage During the Rapid Commutation of a Vacuum Arc. p. 181-188, IEEE.

[8] Childs, S. E., Greenwood, A. N. (1980). A Model for DC. Interruption in Diffuse Mode, *IEEE Trans. Plasma Sci*, vol. ps-8, p. 289-294, (December).

[9] Park, S., Jahns, T. M. (2003). Flexible du/dt and di/dt Control Method for Insulated Gate Power Switches, *IEEE Tran. on Industry Applications*, 39 (3) 0093-9994 (May).

[10] Merz, W., Grims, M. (2012). Fast Opening Switch for High-Voltage Vacuum Tube Protection Application, 2012 *IEEE International Power Modulator and High Voltage Conference (IPMHVC)*, p. 308-311.

[11] Jian, Z., Zhuang, J., Wang, C., Wu, J., Liu, L. (2011). Simulation Analysis and Design of a High Speed Mechanical Contact Base on Electro-magnetic Repulsion Mechanism, *Diangong Jishu Xuebao/Transactions of China Electrotechnical Society*, 26 (8) 1-5, (August).

[12] Sayed, A. H. E., Ker Kennar, R. W. P., Atmadj, A. M. S. (1999). Modeling the Opening Mode of a Fast Acting Electro-Dynamic Circuit Breaker Drive(C), *In*: Proceeding of the University Power Engineering Conference, Leicester, UK, p. 168-172.

[13] Ahn, K. Y., Kim, S. H. (2001). Modeling and Analysis of a High – Speed Circuit Breaker Mechanism with a Spring – Actuated Cam (J), *In*: Proceedings of the Institute of Mechanical Engineers, Part C, p. 663-672.

[14] Lou, J., Li, Q.-M., Sun, Q.-S., Liu, W.-D., Qian, J.-L. (2005). Dynamic Characteristics Simulation and Optimal Design of the Fast Electromagnetic Repulsion Mechanism, *Zhongguo Dianji Gongcheng Xuebao/Proceedings of the CSEE*, 25 (6) 23-29.

[15] Genji, T., Nakamura, O., Isozaki, M. (1994). 400V Class High Speed Current Limiting Circuit Breaker for Electric Power System, *IEEE Trans. on Power System*, 9 (3) 1428-1435.

[16] Hui, D., Wang, Z. K., Zhang, J. Y. (2006). Develpoment and Test 10.5KV/1.5KA HTS Fault Current Limiter, *IEEE Trans. on Applied Superconductivity*, 16 (2) 687-690.

[17] Coqueny, G., Lallemand, R., Josse, G. (2005). Current Limiter Device for Railway and Distribution Network Design and Tests on Railway Conditions 1000A-25KV-50Hz(c), *EPE* 2005, p. 1-7.